CHARACTERIZATION OF
URANIUM SOLIDS PRECIPITATED WITH ALUMINOSILICATES

M. C. Duff*, D. B. Hunter, L. N. Oji, W. R. Wilmarth
Westinghouse Savannah River Company
Savannah River Technology Center, Aiken, SC 29808

At the Savannah River Site (SRS), the High-Level Waste (HLW) Tank Farms store and process high-level liquid radioactive wastes from the Canyons and recycle water from the Defense Waste Processing Facility. The waste is concentrated using evaporators to minimize the volume of space required for HLW storage. Recently, the 2H Evaporator was shutdown due to the crystallization of sodium aluminosilicate (NAS) solids (such as cancrinite and sodalite) that contained close to 10 weight percent of elementally-enriched uranium (U). Prior to extensive cleaning, the evaporator deposits resided on the evaporator walls and other exposed internal surfaces within the evaporator pot. Our goal is to support the basis for the continued safe operation of SRS evaporators and to gain more information that could be used to help mitigate U accumulation during evaporator operation.

To learn more about the interaction between U(VI) and NAS in HLW salt solutions, we performed several fundamental studies to examine the mechanisms of U accumulation with NAS in highly caustic solutions. This larger group of studies focused on the following processes: co-precipitation/structural incorporation, sorption, and precipitation (with or without NAS), which will be reviewed in this presentation. We will present and discuss local atomic structural characterization data about U that has been co-precipitated with NAS solids (such as amorphous zeolite precursor material and sodalite or $Na_8(AlSiO_4)_6 \cdot nH_2O_{(s)}$) using X-ray absorption fine-structure (XAFS) spectroscopic techniques.

Our results indicate that U uptake from solution is greater during the precipitation of sodalite and amorphous zeolite precursor material than during the precipitation of zeolite A and amorphous zeolite. The XAFS data indicate that U exists in several forms, such as U(VI) (uranyl- and uranate-type) oxide and oxyhydroxides (such as clarkeite). Crystalline forms of U(VI)-silicate were not resolved from the XAFS spectra but the presence of Si in the outer coordination shell of U indicate that the U is probably associated with amorphous silica. Mass balance determinations for U in these materials indicate that during formation, the structural incorporation of U within these structures is not a likely mechanism for accumulation. However, uptake of U was greatest during the precipitation of amorphous zeolite precursor material. Additionally, removal of U from solution by surface sorption on the NAS solids (a process which could have occurred after these solids were formed) probably had a minor role with respect to U accumulation in the 2H Evaporator. Processes most likely to largely influence on U accumulation are precipitation as U(VI) (as uranyl/uranate) oxide/oxyhydroxides and formation of an amorphous U-silica material.

INTRODUCTION

Uranium accumulation during the evaporation of HLW is a potential criticality risk if the incoming waste is enriched in [235]U. Little is known about the interactions between U and NAS in caustic, high Na^+ HLW salt solutions at room and at elevated temperature. To examine these interactions during NAS formation, we conducted studies that focused on potential mechanisms of U accumulation with NAS in the evaporators and in other process areas at the SRS that may concentrate U in the presence of silicates, Al and NAS. It is intended that the information gained from these studies will help support the basis for the continued safe operation of SRS evaporators and that this fundamental information will be used to help mitigate U accumulation during evaporator operation.

Potential Routes of U Accumulation with NAS

During the evaporation of caustic Na^+-rich solutions, several processes could potentially contribute to the accumulation of U-containing solids. Uptake processes by solids can occur by several mechanisms: structural incorporation, ion exchange (electrostatic or outer-sphere) sorption, specific adsorption and surface precipitation/polymerization. **Figure 1A-D** demonstrates potential U interactions with NAS on the molecular scale,

which is the scale in which XAFS structural information is obtained.   Typically, the expression of these uptake processes depends upon the amount of metal added, solution and solid phase characteristics [1, 2].

Many of the terms used to describe these processes have been used loosely in the literature and their use varies with scientific discipline. For example, "Ion exchange" can have different meanings. One method to express ion
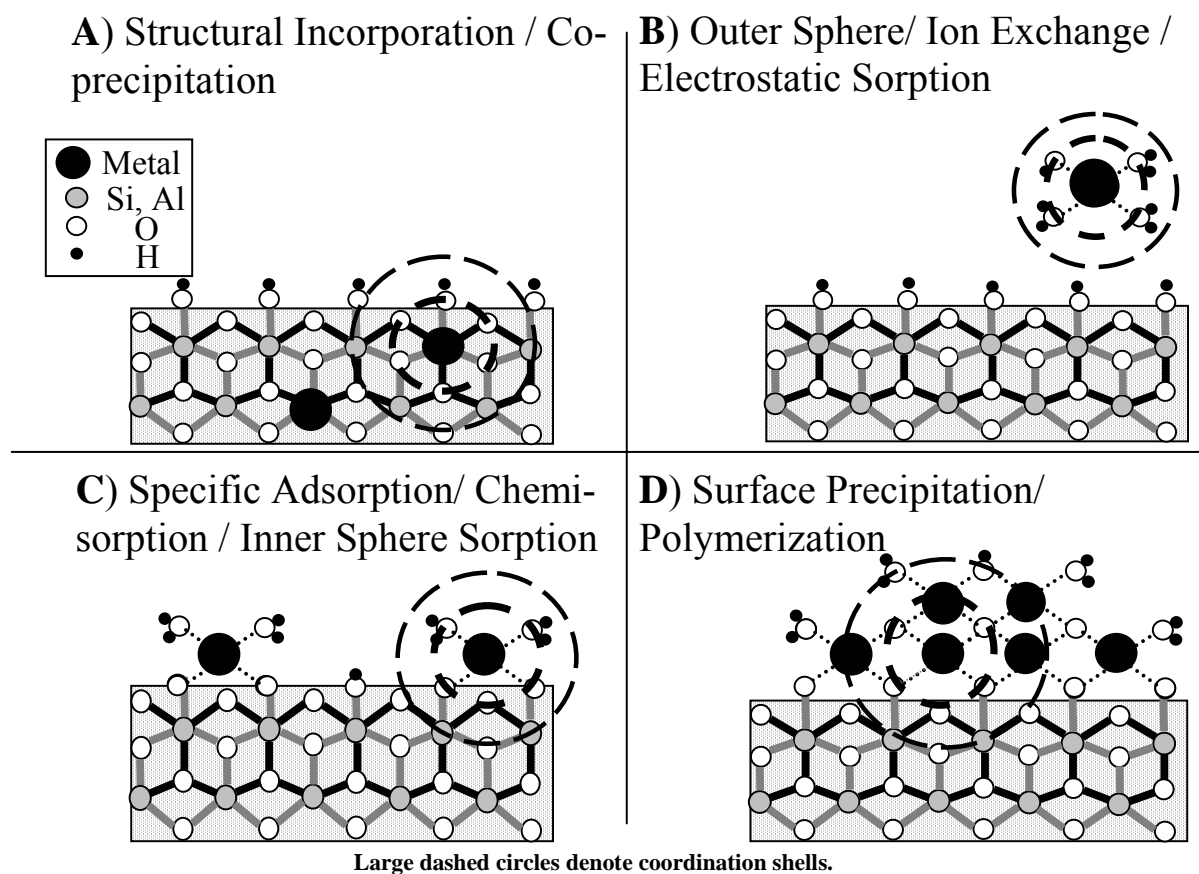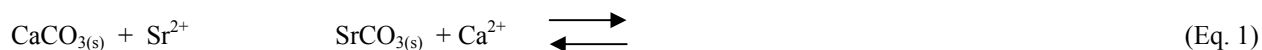
A) Structural Incorporation / Co-precipitation

B) Outer Sphere/ Ion Exchange / Electrostatic Sorption

C) Specific Adsorption/ Chemi-sorption / Inner Sphere Sorption

D) Surface Precipitation/ Polymerization

Large dashed circles denote coordination shells.

Fig. 1 Simplified diagram of the types of associations a metal could have with a surface: **A**) Structural incorporation/co-precipitation, **B**) Outer-sphere (electrostatic) sorption, **C**) Specific or inner-sphere sorption and **D**) Surface precipitation. Dashed rings denote first, second and third shell environments that can be probed with X-ray absorption fine-structure (XAFS) spectroscopic techniques.

exchange is Structural Incorporation, which is the substitution of a solution species for a structural atom as shown in the example below for strontium (Sr) ion substitution for calcium (Ca) ion in calcium carbonate or $CaCO_{3(s)}$.

$$CaCO_{3(s)} + Sr^{2+} \rightleftharpoons SrCO_{3(s)} + Ca^{2+} \qquad \text{(Eq. 1)}$$

This type of metal uptake typically requires ready access to structural atoms. An example of this process would be the exchange of Na^+ for Ca^{2+} within the interlayer region of a layered metal oxide material. Structural incorporation includes co-precipitation, where a new atom substitutes for host structural atoms during the formation of the host solid.   Ideally, structural incorporation of anions could also occur.   Therefore, the local environment of the exchanged atom(s) would resemble the environment that of the newly exchanged atom prior to its release into solution (**Fig. 1A**). Two exceptions to this would be when the host structure is a nanoparticle (i.e., of vary small dimension) and when the structure is amorphous or structure-less. In these cases, exact determinations of whether the participating metal species resides in a structural vacancy or within an interlayer site are not straightforward (**a**).

(**a**) Due to the small nature of nanoparticles, they often have more atoms at the solid-water interface than inside the solid. The use of spectroscopic techniques to elucidate the exact location of sorbing metals in such solids may potentially result in an inability to determine whether the metal is in an interlayer, surface or vacancy site.

Ion Exchange in a more restrictive sense as used in this study is an electrostatic process involving the replacement of one readily exchangeable hydrated ion by another similarly exchangeable ion (**Fig. 1B**). This type of sorption is also referred to in the literature as Outer Sphere sorption. It does not involve the formation of bonds with the participating surface because the sorbed ion is only present in the diffuse double layer (DDL). Outer sphere sorption is normally reversible (**b**) and is a function of ionic strength (i.e., such as Na^+ ion concentration). Ion exchange sorption is often associated with materials that have constant surface charge and exhibit no change in overall surface charge upon ion exchange sorption. An example of this process would be exchange of two hydrated Na^+ ions for one hydrated UO_2^{2+} ion (also called the uranyl ion) in the DDL.

Specific Adsorption (often referred to as Chemisorption or Inner Sphere sorption) involves the formation of predominantly covalent bonds with the surface, but the bonds can have some ionic behavior. These adsorbed metals typically have one or more atoms from the participating surface in the second coordination shell (**Fig. 1C**). This type of sorption involves the release of H^+ or structural surface ions (such as Na^+ in monosodium titanate or MST) upon sorption. For example, specific sorption of UO_2^{2+} to NAS could result in the presence of Si and Al atoms in the second coordination shell of the UO_2^{2+}. Specific adsorption is usually irreversible [(**c**)]. However, in the literature, specific adsorption is not always differentiated from structural incorporation or surface precipitation. Specific adsorption may involve mononuclear complexes or polymeric species. It may occur with metals and their associated ligands [such as a U(VI)-carbonate ion] and it is influenced by other solution- and surface-related variables (**c**).

Surface Precipitation occurs by nucleation of new solid phase on a host surface (**Fig. 1D**). For example, when the concentration of a dissolved metal such as UO_2^{2+} is high enough to result in the super-saturation of one or more UO_2^{2+}-containing phases [such as schoepite, which has a formula of $U(VI)O_3 \cdot 2H_2O_{(s)}$] in the presence of another solid, the other solid may facilitate the nucleation of a new solid UO_2^{2+}-rich phase. This U-rich material would have numerous U atoms in the second or third coordination shell of the U. The formation of colloidal (polymeric) U species on surfaces could resemble the same local environment (on the atom scale) as observed for surface precipitation. When atoms from a potential host surface are absent and polymeric species are present, the mechanism of U uptake from solution is likely to be direct homogeneous (solid phase) precipitation.

In HLW, U may be concentrated by sorption to the surfaces of the NAS, precipitation within NAS structures and precipitation as U phases. Sorption can be divided into two types of molecular scale processes (outer sphere and specific adsorption) that involve the uptake of atoms near or at a participating sorptive surface. An element such as U could co-precipitate with the NAS and related solids. [For zeolites, the term co-precipitation could be further divided to include uptake into zeolite channels and any isomorphic substitution (i.e., of U for Si or Al) in the zeolite structure [3]. The U could also deposit by precipitation via surface nucleation (often referred to as chemical seeding) on NAS minerals. It is also possible that U solids could seed the growth of NAS solids. The U could

(**b**) Sorption reversibility is tested by leaching the metal loaded solid with a target metal-free solution that has the same properties (i.e. ionic strength, background electrolytes, pH etc…) and measuring the leachate solution to determine whether any target metal is released. Specifically adsorbed species are typically not leached with lower ionic strength solutions and specific adsorption processes are not a function ionic strength (assuming the electrolytes do not interact with the sorbed species via complexation etc.). Outer-sphere species can be readily removed with solutions of low ionic strength or solutions that contain high concentrations of a cation that has a higher affinity for the surface than the outer-sphere species. Therefore, outer-sphere sorption is viewed as reversible and a function of ionic strength.

(**c**) Specific adsorption is typically a function of surface charge properties. When a participating surface has a charge that varies with solution pH, specific adsorption exhibits pH-dependent behavior. For example, a surface that is highly protonated (at low pH) will have more affinity for negatively-charged species. As the pH decreases, the surface charge of pH-dependent charged surface becomes more negative and the uptake of positively charged species is favored. Therefore, the surface of metal oxides for example specifically adsorbs more positively charged species as the solution pH increases. However, this behavior is generalized. As the solution pH increases sorbing species undergoes a change in speciation—such as hydrolysis. In this case, the amount of specific adsorption becomes a function of solution speciation. Ion exchange resins that sorb free ions of actinides (e.g., the non-hydrolyzed Pu^{4+} species) at high H^+ concentrations (i.e., low pH) will release sorbed Pu^{4+} species when the solution

pH is raised—due to the hydrolysis of the sorbed Pu^{4+} (e.g., $Pu(OH)_3^+$, $Pu(OH)_2^{2+}$). The hydrolysis species have a lower overall charge and their size (as an ion group) is larger than the free ion—making them have a lower affinity for the surface. Other processes [particularly for U(VI)] that can influence sorption are metal complexation with ligands (i.e., with carbonate ion) or in the case of anions, protonation (e.g., $PO_4^{3-} + H^+ \rightarrow HPO_4^{2-}$). Specific adsorption processes are a function of many variables. potentially precipitate as an oxide [e.g., $UO_{3(s)}$], a hydrous oxide [e.g., $Na_2(UO_2)_3O_3 \cdot (OH)_{2(s)}$], and a silicate [e.g., [e.g., $Na_4(UO_2)_2(Si_4O_{10})_4 \cdot 4H_2O_{(s)}$] (d) [4].

Uranium may also interact with silica sols, which have no defined crystal structure because of their amorphous nature. At an atom- or molecular- scale basis, this type of interaction with U may be best be described by structural incorporation in **Fig. 1A**, which shows U in a crystalline structural-type environment. However, from a XAFS point of reference, the local environment of U that is associated U with amorphous silica would not resemble that of a crystalline U silicate structure.

Review of U(VI) Chemistry and Uptake Studies with U(VI) and Zeolites
In oxidized systems, dissolved U exists as the highly soluble uranyl $[U(VI)O_2^{2+}]$ species with two axial U=O double bonds at ~1.75 to 1.8 Å. This form of U(VI) can exist in U solids and in solution. However, U(VI) can also exist in solids as the less common uranate form, which has at least three single U-O bonds and no short axial double bonds. Several solid phases or sorbents such as the titanates (such as monosodium titanate or MST) and Mn oxides will concentrate U and other radionuclides under conditions that are similar to alkaline HLW salt solutions [5, 6, 7, 8]. At high pH, the surfaces of most solids are negatively charged and likely to sorb cationic species, such as Sr^{2+}. Under these solution conditions most actinides such as U(VI) exist as negatively charged hydrolysis, carbonate (CO_3^{2-}) [such as $(UO_2)_2(OH)_5^-$ and $UO_2(CO_3)_3^{4-}$] and possibly nitrate species [9]. When these U(VI) species dominate the solution speciation (at high pH or in high CO_3^{2-} or NO_3^- solutions), U(VI) typically has a low affinity for certain solids, like the Fe oxides [10-11]. The sorption of U(VI) species among other actinide species on sorbents such as the titanates occurs to a limited extent at high pH. The mechanisms by which these processes occur are known to some extent in that specific adsorption of mono and dimeric uranyl species occurs on the MST [12]. Sorption studies with U(VI) typically demonstrate that it has low affinity for zeolites at high pH (9 to 11)— particularly with high levels of dissolved CO_3^{2-} [13, 14, 15, 16]. This is because high levels of dissolved CO_3^{2-} favor the formation of negatively-charged, highly soluble U(VI)-carbonate complexes, which have low affinities for similarly-charged surfaces. Few sorption studies have been done with U and zeolites above pH 12. Studies that have synthesized zeolites in the presence of U(VI) under acidic conditions show that uptake can occur and result in deformities within the zeolite structure. Under acidic conditions, these deformities permit U uptake at locations that would normally have Na^+ or H^+ ions—depending on the form (i.e., Na^+ or H^+) of the zeolite [3]. Other studies that have examined the uptake of U from highly acidic solutions that are precipitating zeolites indicate that the U is in dimeric cavities of the zeolites as hydrated forms such as $[UO_2(OH)_4]^{2-}$ [17].

Use of XAFS Techniques to Characterize Metal Uptake by Surfaces
The local environment of metals associated with surfaces can be investigated with analytical techniques such as XAFS spectroscopy. It is an X-ray-based technique that is non-destructive and provides average information on bulk and surface behavior. The XAFS spectroscopic techniques are among the best for providing detailed chemical speciation information in environmental samples—particularly when information from multiple characterization techniques is available. The term XAFS is applicable to both X-ray absorption near-edge structure (XANES) and extended X-ray absorption fine-structure (EXAFS) spectroscopic techniques. XAFS spectra give robust local structural information on coordination number (CN), bonding symmetry, neighbor and near-neighbor atomic distances and bond disorder (as the root mean square deviations of distances about the average values). Additionally, the information gained is atom specific—making it a versatile technique for structural determinations of atom clusters [18, 19]. XAFS spectroscopy has been applied to the structural elucidation of metal clusters and sorbed metals on surfaces because the technique does not require long range order (i.e., periodicity) or crystalline samples. Hence, this technique can characterize colloidal forms of ions and species that would otherwise be undetected by XRD because of their poorly crystalline behavior.

Experimental Objectives
The primary objective of this research was to obtain information on speciation of U [added as U(VI)] associated with NAS solids that were synthesized with dissolved U using XAFS. Uranium-XAFS analyses were also

(**d**) No U-aluminate solid phases have been documented. If these phases form, other U phases, such as the oxides, hydroxides and silicates of U are more likely dominate the speciation of solid phase U under evaporator and salt solution conditions.

conducted on solids that had been washed with solutions of DI water (only) and after washing with DI water and Na_2CO_3. Washing U-loaded solids with Na_2CO_3 solutions has been shown to remove sorbed forms of U(VI), in addition to dissolving the readily soluble (i.e., rapidly dissolving) solid phase forms of U(VI) [20]. This is due to the formation of highly soluble U(VI)-carbonate complexes, such as the U(VI) di- and tri-carbonato species, which typically have low affinities for sorbents, such as the aluminosilicates [21] and metal oxides [11]. We used XAFS techniques to obtain information on the average local structural speciation of the U such as CN, geometry, near and next nearest neighbor environment of the target metal. To determine whether our results were realistic, we used molecular models to evaluate the findings from our XAFS studies.

MATERIALS AND EXPERIMENTAL METHODS

Sample Preparation

The NAS solids (amorphous zeolite, sodalite and zeolite A) were synthesized according to modified methods supplied by A. Mensah of the Univ. of South Australia. Details of the syntheses and the solids characterization are reported by Mensah et al. (2002) and Oji and Williams (2002) [22, 23]. The amorphous zeolite and sodalite were each synthesized in 0.4 M Al and 0.4 M Si solutions in 4.0 M NaOH whereas the zeolite A was synthesized in 0.29 M Si and 0.29 M Al solutions in 4.7 M NaOH. All solids were synthesized in one-L solutions in the presence of 50 mg of U(VI). The difference between the amorphous zeolite and sodalite syntheses was temperature, in that the amorphous zeolite was made at 40 ^{o}C and the sodalite was made at 80 ^{o}C. Zeolite A was made at 90 ^{o}C. After preparation, the solids were washed three times in DI water, filtered with a 0.25   m nylon filter, and dried in air. The air-dried solids were then washed three times with 0.4 M Na_2CO_3, filtered with a 0.25   m nylon filter, and then air-dried. The air-dried solids were analyzed using XAFS techniques. Sub-samples of the solids were digested in acid to determine the U concentrations after synthesis (using inductively-coupled argon plasma mass spectrometry) after each of the two washing steps. The results of the sample digests are shown in **Table 1**. Washing of the U-NAS solids with DI water and Na_2CO_3 solutions resulted in the removal of salts and some NAS material. Hence, in most cases, more NAS was removed by washing (on a % basis) than the U. This preferential removal of U resulted in higher U concentrations (U enrichment) in the solids after washing—for the amorphous zeolite and the sodalite samples. The washes of the U-NAS solids were performed to determine the lability of the U that was associated with the NAS solids and to investigate the speciation of U in the resultant washed material. With washing, the more labile (i.e., readily soluble or rapidly dissolving and desorbed U) forms of U are removed, leaving the more stable (less soluble or kinetically slow to dissolve) forms of U in the solid phase. It was anticipated that by selectively washing/leaching various types of U from the solids, a more homogeneous population of U species would be left in the washed solids. These U-NAS precipitates did not exhibit any XRD patterns indicative of known U solids [23] so XAFS was a suitable technique to use for the characterization of these solids.

Table 1. Concentrations of U associated with the synthetic NAS solids and reference materials

Sample Description	U Concentration (mg U kg^{-1} solid after preparation or after washing)
Unwashed Amorphous Zeolite Material	280
DI Water Washed Amorphous Zeolite Material	490
Na_2CO_3-Washed Amorphous Zeolite Material	Not determined
Unwashed Sodalite	820
DI Water Washed Sodalite	1,500
Na_2CO_3-Washed Sodalite	Not determined
Unwashed Zeolite A	180*
DI Water Washed Zeolite A	110*
Na_2CO_3-Washed Zeolite A	Not determined
U Reference Solid for Amorphous Zeolite	Not determined**
U Reference Solid for Sodalite	Not determined
U Reference Solid for Zeolite A	Not determined

*   The U concentrations in the Zeolite A samples were too low for characterization using XAFS.

** Although not determined, we estimate these solids contained several %U based on the high U-XAFS signal that we obtained for them.

Additionally, to determine when the U should be added during these NAS syntheses, precipitation timing studies were done with U, Al and caustic salt solutions using the same experimental conditions (such as temperature) as those required for the individual NAS syntheses [i.e., the reference samples as listed in 23]. No Si was added to avoid making NAS for each of these reference U materials. The U added to these solutions underwent precipitation and the unwashed solids were supplied for XAFS analyses. The solids in these "reference" samples may be representative of solids that can form in heated caustic solutions that are low in Si but contain high Al.

EXAFS Data Collection and Analyses
The XAFS data were collected on beamline X23a2 at the National Synchrotron Light Source (NSLS, Brookhaven National Laboratory, Upton, NY). Uranium-XAFS data were collected at the U L_3-edge (17,166 eV) on the air-dried filtered U-containing NAS solids. The XAFS data were collected in fluorescence mode using an unfocussed X-ray beam and a fixed-exit Si(311) monochromator. Ion chambers were used to collect incident (*Io*), transmission (*It*) and reference (*Ir*) signals. Gas ratios in *Io* were 100 % Ar. A Lytle detector was used to collect fluorescence X-rays (*If*). The monochromator energy was maximized using a piezo stack feedback energy stabilization system, with a settling time of 0.3 seconds per change in energy. An X-ray beam size of 2 by 28 mm^2 was used. Energy calibration was done using foils of Pt (L_1-edge of 13,880 eV), Zr (K-edge, 17,998 eV), and Mo (K-edge, 20,000 eV).

In simple terms, chi data (the plot of the wavevector in reciprocal space) show the oscillatory component (with both constructive and destructive interferences) of the atoms in the neighbor environment of the element of interest. The chi data represent part of the photoelectron wave that can be defined by the EXAFS equation [18, 19]. The EXAFS equation is shown in a highly simplified form below:

$$\text{Chi(k)} = \frac{F(k)*N*S}{k*R^2}\; S_0^2 e^{(-2*k^3\sigma^2)} \sin[2*k*R + \delta(K)]. \tag{Eq. 2}$$

Chi of k is the square root of $[(2m / \hbar^2) * (E - E_0)]$. S_0^2 is the amplitude reduction factor, which is associated with central atom shake-up and shake-off effects. SIGMA^2 or σ^2 is the Debye-Waller Factor or Relative Mean Square Disorder in bond length. "$\hbar$" is Plank's constant and R pertains to mean atom position or radial distance in Å. "m" is the mass of the photoelectron, E_0 is the EXAFS defined edge energy in electron volts or eV (not equal to edge energy as defined by XANES but is equal to the energy of the photoelectron at $k = 0$. "F of k" is the backscattering amplitude of the atom. N is the coordination number and $\delta(K)$ represents the electronic phase shifts due to atomic potentials.

The background contribution to the EXAFS spectra was removed using an algorithm (AUTOBK) developed by Newville et al. (1993), which minimizes R-space values in low k-space. Each chi data set was read into the WINXAS analysis package [24, 25]. Replicate scans were co-added to improve S/N. The U-XAFS spectra were analyzed from 2 to 12 Å^{-1}. The chi data were k^3-weighted and Fourier-transformed (FT) to yield R-space or Radial Distribution Function (RDF) plots [26]. Simulated EXAFS spectra were also generated based on the documented crystallographic properties for U(VI)-silicate and U(VI)-oxyhydroxide solids using ab initio based theory, which involved FEFF 7.2 a program created by researchers at the Univ. of Washington [27, 28, 29, 30, 31]. Model fits for U were performed in R-space.

RESULTS

Background on the XAFS Characterization of Behavior of U on Surfaces
The XAFS techniques have been applied to the study of U(VI) on a variety of solids, such as Fe oxides, carbonates, silicates and sulfides [32, 33, 34, 35, 36, 37, 38, 39, 40] and within mineral oxides, calcite, oxyhydroxides and gels [41, 42, 43, 44, 45]. Most of these studies have an environmental focus because they were performed with naturally-occurring minerals under conditions relevant to the geologic surface and subsurface environments. The findings of these studies vary greatly but they typically indicate that sorbed UO_2^{2+} species (in the absence of a redox-active mineral surface) form inner sphere bonds with the sorbent solids over a solution pH range between 5 to 12 via primarily edge-linking with octahedral or tetrahedral structural components. Corner-linking in addition to edge-linking of sorbed U with silica tetrahedral is observed at the muscovite surface however, this aluminosilicate has a difference structure than that of zeolites. Surface sorption sites on zeolites offer corner-linking sites through

single terminal O atoms, as opposed to edge linking sites (as with muscovite), which offer edge-linking via two O atoms.

The U(VI)-complexes that have been observed on surfaces using XAFS techniques are typically monomeric U(VI)-hydroxo and U(VI)-carbonato species that form mono- and bidentate linkages with the participating surfaces (as noted in **Fig. 2A**). In acidic solutions, some U(VI) species sorb mainly via an outer sphere mechanism on some silicates. Dimeric U(VI) species are also observed. XAFS and wet chemical studies have elucidated that U(VI) sorbs on broken edge sites of layered smectitic (aluminosilicate clay) minerals. These aluminosilicate minerals typically sorb cations such as Na^+ and Ca^{2+}, which form outer sphere (electrostatic) surface complexes on the fixed charge sites of basal planes of edge-sharing Al octahedra and edge-sharing Si tetrahedra as shown in **Fig. 2A** (**e**).

The broken edge sites of these minerals, which possess pH-dependent charge are thought to host the sorption of U(VI) species [46, 47]. In contrast, XAFS and XRD crystallographic studies have shown that uranyl silicate minerals such as soddyite $[(UO_2)_2SiO_4 \cdot 2H_2O]$, $Na_4(UO_2)_2Si_4O_{10} \cdot 4H_2O_{(s)}$, Na-boltwoodite $[Na_2(UO_2)_2 (SiO_3OH)_2 \cdot 1.5H_2O]$ and Na-weeksite $[Na_2(UO_2)_2(Si_5O_{13})_6 \cdot 3H_2O]$ possess predominantly corner-sharing behavior as opposed to edge-sharing behavior between U polyhedra and silica tetrahedra as shown in **Fig. 2A** [4, 48, 49]. The local environment of sorbed U(VI) on muscovite was described using U-XAFS data and modeled by Moyes et al. (2000) [32]. They observed edge-sharing between the uranyl and a Si tetrahedron (i.e., the shortest U-Si radial distance). The longer U-Si distance was obtained by positioning a second neighboring corner-sharing Si tetrahedron next to the first edge-sharing Si tetrahedron. Hence, the bonding of uranyl was primarily through the edge-sharing Si tetrahedron that was also bonded to another Si tetrahedron. In slight contrast to these studies with crystalline muscovite, are the non-XAFS–based calculations of U(VI) that is sorbed to amorphous Si [50]. These theoretical studies showed that that the more energetically favorable association of U at low loadings on amorphous silica gel (at 500 mg U per kg silica) could be via edge-sharing with silica at U-Si radial distances of less than 2.93 Å. These results were consistent with work by Reich and researchers [51]. At higher surface loadings, (>500 mg U per kg silica), these calculations predicted bonding via corner-linking of uranyl species with silica tetrahedral at radial distances of 3.54 Å or greater. Other spectroscopic studies with silicate gels indicate that U sorbs via edge-sharing with silica tetrahedral [52]. This type of sorption to surface via edge-linking (as opposed to corner-linking) is common for sorbed U(VI) species [20, 40].

Little if any experimental XAFS work has been done with dissolved, sorbed or precipitated U species under conditions relevant to that of HLW solutions. Hexavalent U(VI) is probably the predominant oxidation state of U in HLW salt solutions. Uranium-XAFS studies have been performed to study the structure of high levels of dissolved U(VI) species under simulated caustic solutions [in 3.5 M tetramethylammonium, which was used as a counterion to suppress the precipitation of U(VI)] [9] and of solid phase U in real HLW samples [53]. These XAFS studies identified that the most common U(VI) complexes in caustic solutions are likely to be the monomeric $UO_2(OH)_4^{2-}$ and $UO_2(OH)_5^-$ species. Our recent studies with U in real HLW sludge indicate that about 95 % of the sludge U exists in the hexavalent U(VI) form whereas about 5 % of the U is metallic [53].

Uranium Chi Data

The k^3-weighted chi spectra for the U in the U reference and the various washed and unwashed U-containing amorphous zeolite precursor materials are shown in Fig. 2B. Additionally, the k^3-weighted chi spectra for the U in the U reference and U-containing amorphous sodalite precursor material are shown in Fig. 2C. The chi data for U

(**e**) Smectite clays are phylloaluminosilicate minerals consisting of layers of aluminum octahedra and silicon tetrahedra that contain metals (such as $Fe^{2+,3+}$, Mn^{2+} and Mg^{2+}) within the structural vacancies. Fixed charge sites on aluminosilicate clays do not exhibit pH-dependent surface charge behavior. These fixed charge sites typically sorb solution ions via an outer sphere/electrostatic mechanism. The fixed charge of the sites comes from an imbalance in internal structural charge due to the substitution of metal ions with a different charge than that which would normally fulfill charge balance in the clay structure (specifically, Al^{3+} and Si^{4+}). On the edges of these structural layers are broken edge sites, which exhibit pH-dependent charge behavior due to their propensity to protonation and deprotonation. It is at these sites that specific adsorption of metals such as uranyl can occur.
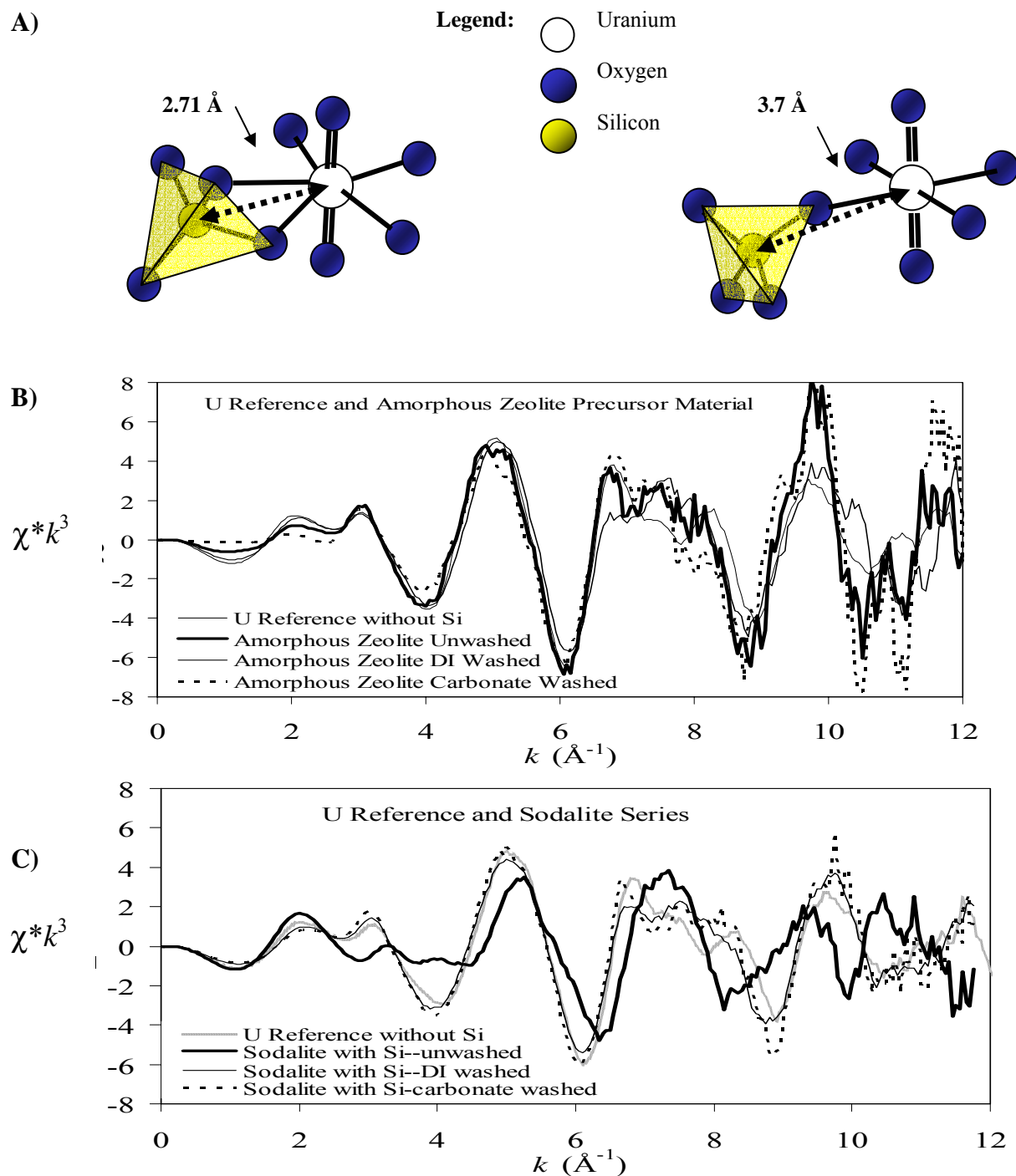
A)

Legend: ○ Uranium

● Oxygen

● Silicon

2.71 Å

3.7 Å

B)

U Reference and Amorphous Zeolite Precursor Material

$\chi*k^3$

— U Reference without Si
— Amorphous Zeolite Unwashed
— Amorphous Zeolite DI Washed
---- Amorphous Zeolite Carbonate Washed

k (Å^{-1})

C)

U Reference and Sodalite Series

$\chi*k^3$

— U Reference without Si
— Sodalite with Si--unwashed
— Sodalite with Si--DI washed
---- Sodalite with Si-carbonate washed

k (Å^{-1})

Figure 2 (A, left) In published U-XAFS literature on uranyl sorption to silica gels, the U-Si distance of ~2.71 Å (dashed arrow) and has been interpreted as edge-sharing. Hence, short U-Si distances without long radial distances are a typical signature for sorption. In published U-EXAFS literature for uranyl silicates, the U-Si distance is ~ 3.7 Å (dashed arrow, **A, right**), which is indicative of corner-sharing. Long U-Si distances typically signify structural incorporation of U (i.e., longer radial distances are needed for a lattice environment as opposed to a sorption-type environment. (**B**) and (**C**) represent chi data for the amorphous zeolite and sodalite series (respectively).

These samples indicate there are light and heavy atom backscatterers as evidenced by the presence of a large amplitude signals at low and high k. With the exception of the unwashed zeolite, the spectra are quite similar. In general, the spectra show many similar features—particularly at low k. However, the chi data for the unwashed sodalite samples differs greatly from the other samples.

Uranium Fourier-Transformed Data
The FT data for the amorphous zeolite series samples are shown in Fig. 3A. For all of the samples, the first coordination shell consists of a split uranyl-type shell that contains O atoms at two different distances. These two first shell peaks represent axial and equatorial U-O bonding behavior as shown pictorially in Fig. 3A. There are significant peaks in the transforms at greater radial distances (i.e., outer shells) for the unwashed and the Na_2CO_3-washed amorphous zeolite precursor solids. The FT data for the DI-washed amorphous zeolite sample and the U reference for the amorphous zeolite synthesis do not possess significant higher shell peaks. The higher coordination shell peaks in the FT data for the Na_2CO_3-washed sample are more pronounced than that for the DI washed and unwashed samples—suggesting that washing removes one (or more) U phases. Hence, washing may result in a material that is more characteristic of a single U phase because the magnitude of FT peaks increases with washing. The lack of strongly defined peaks in the 3 to 4 Å region of the unwashed and DI-washed amorphous zeolite sample spectra is characteristic of the uranyl oxide hydrate called schoepite $[U(VI)O_3 \cdot 2H_2O_{(s)}]$ [41]. The XAFS spectra for U-U interactions in schoepite are representative of multiple environments, which results in decreased peak heights in the FT data for the outer shell U-U interactions. However, it is difficult to interpret XAFS spectra that are representative of multiple species.

The FT data for the sodalite series samples are shown in Fig. 3B. Three of the samples contain a typical split first shell environment for uranyl (much like that described for some of the previous samples). These two first shell peaks are indicative of uranyl behavior. The FT data for the fourth sample (the unwashed sodalite sample) contains three peaks in the first coordination shell. The additional (middle distance) peak is indicative of uranate-type behavior as opposed to uranyl-type behavior. Uranate-type bonding behavior is less common than that of uranyl bonding behavior [20, 54, 55]. Additionally, uranate-type bonding is not common to all uranate-named solids. Some uranate-named solids possess uranyl behavior and some do not (**f**). For example, it is thought that sodium diuranate and clarkeite have a split first shell (like that of uranyl) with equatorial and axial O's. However, these phases have long axial O's distances (near 1.9 Å) relative to traditional axial O distances at 1.75 to 1.8 Å [54]. This feature is somewhat consistent with typical uranyl-containing solids and solution complexes. [Note: Clarkeite $[Na[(UO_2)O(OH)](H_2O)_{0-1}]$ is a partially hydrated form of sodium diuranate that possesses uranyl-type bonding [55]].

As was observed with the FT data from the amorphous zeolite U reference spectra, the outer shell peaks in the FT data for the Na_2CO_3-washed sodalite sample are more pronounced than that for the DI-washed and unwashed sodalite samples—suggesting that washing removes one (or more) U phases. Hence, washing may result in a U solid that is more characteristic of a single U phase because the magnitude of FT peaks increases with washing.

Uranium FT Model Fit Data
Due to the presence of multiple local environments in most of the XAFS spectra for the U samples, fits were only performed with the spectra for the reference samples and the two Na_2CO_3-washed amorphous zeolite and sodalite samples. The complexities associated with XAFS analyses for samples with multiple environments will be discussed in the following sections. XAFS analyses provide average coordination and bonding environment information and they typically cannot provide information on population distributions of species.

The FT data and corresponding first and second shell fit data for the Na_2CO_3-washed amorphous zeolite sample indicate that this solid has one set of uranyl-type axial O atoms at 1.79 Å and three equatorial O atoms at 2.42 Å (data not shown). A CN of three for the equatorial O atoms is fairly low, based on typical literature values.

Attempts to fit for a higher number of equatorial O atoms were unsuccessful. The FT data for the outer shells contains two Si atoms at a U-Si radial distance of 3.60 Å and three Si atoms at a U-Si radial distance of 3.92 Å (Fig. 4A). These long radial distances are indicative of Si corner-sharing behavior with U polyhedra as previously discussed. Two outer shell U atoms were also identified to exist at 3.92 Å. Collectively, these data indicate that a uranyl silicate phase or phases are present in the carbonate-washed amorphous zeolite precursor sample (**g**).

(**f**) A discussion of the uranate structures and misclassifications is an important topic but such discussion is not warranted in this report given the results that will be discussed.

(**g**) Because of its similar size, Al may be present instead of Si, but to date, no crystalline uranyl aluminate solids have been identified, suggesting that bonding to Si is much more likely than to Al.
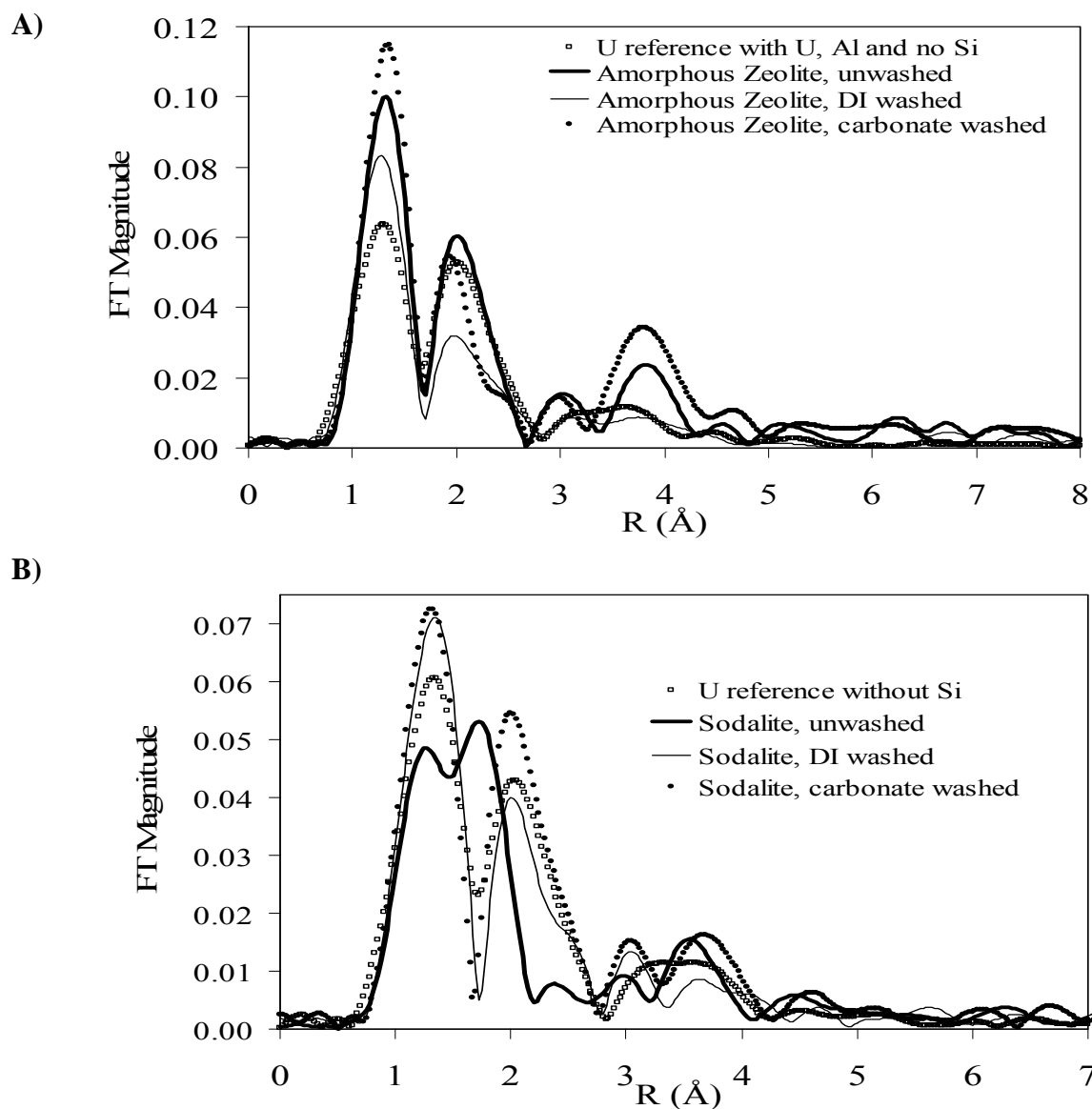
A)

B)

Fig. 3 FT data for the (**A**) amorphous zeolite and (**B**) sodalite series samples—uncorrected for phase shift.

The FT data and corresponding first shell fit data for the carbonate-washed sodalite sample indicate the U in this solid has on average one set of three uranyl-type axial O atoms at 1.77 Å and six equatorial O atoms at 2.47 Å. A value of three O atoms at a single axial U-O distance is one CN too high (a CN of two is physically ideal for uranyl-type U). These results do not indicate that there are two different U phases. Our XAFS fits provide average values and if there were two sets of uranyl phases (specifically, axial O atoms at two different distances) we would expect to obtain a total CN (i.e., sum) of two for these O atoms. More suitable fits for the first shell axial O atoms were not possible.

The FT data for the outer shells (data not shown) contains three Si atoms at a U-Si radial distance of 3.61 Å, which is a distance indicative of Si corner-sharing behavior with U polyhedra as previously discussed (shown in Fig. 4B). A multiple scattering between two uranyl axial O atoms at 1.8 Å can occur at 3.61 Å but our fits indicate that this feature plays a minor role in the FT data. Three U atoms at a U-U radial distance of 3.86 Å were also observed. Collectively, these data indicate that a uranyl silicate phase or phases are present in this Na_2CO_3-washed sodalite sample. These U-U model fit data are not representative of uranate phases, which have much longer U-U radial distances (e.g., 6 Å for a cobalt uranate).

The FT data and corresponding first shell fit data for the Si-free U reference solid (for the amorphous zeolite synthesis, data not shown). The U in this sample has two sets of uranyl-type O atoms at 1.76 Å and 1.88 Å and five equatorial O atoms at 2.42 Å. Fits performed with a single set of axial type U-O interactions were not successful. We recognize that having four axial O atoms at two different distances is uncommon to most U solids. The complexities associated with these fits suggest that more than three environments exist for the local coordination of U in this sample. Hence, fits for interactions for higher shells were not performed due to the multiple local environments.

The FT data and corresponding first shell fit data for the Si-free U reference solid (for the sodalite synthesis) are (data not shown) were much like that for the Si-free amorphous zeolite samples. The U in this solid has two sets of uranyl-type axial O atoms at 1.76 Å and 1.87 Å and four equatorial O atoms at 2.40 Å. These first shell data are similar to that obtained for the U reference solid as discussed previously. Fits that were performed using a single set of axial type U-O interactions were unsuccessful. Again, we recognize that having four axial O atoms at two different distances is uncommon to most U solids. The complexities associated with these fits suggest that multiple environments exist for the local coordination environment of U in this sample.

Fits were successfully performed for the second shell interactions in the U reference solid from the sodalite syntheses. The fits indicate the presence of one Al atom in the outer shell at 3.60 Å (based on using Si, which is a good analog for Al because it has a similar mass to that of Al) in addition to three U atoms at 3.83 Å (data not shown). These data suggest that a U(VI)-aluminate solid phase may be present in this sample. Aging studies conducted by SRTC researchers have been conducted to examine U(VI) solubility in HLW simulant solutions over a large range of hydroxide, nitrate, nitrite, and aluminate concentrations—in addition to two temperatures (room temperature and 85°C) [56, 57]. These studies did not attribute U solubility to be strongly influenced by aluminate concentration. Decreases in aluminate levels were attributed to the precipitation of Al-containing solids (such as gibbsite). Some of the decreases in U solubility that were observed were thought to be due to multiple component effects, which could not be statistically isolated. However, Al concentration was used in the predictive U solubility equations that were generated in these studies. The solids from these studies were not isolated and characterized. Additional work is recommended to investigate the influence of Al on U solubility and the local coordination environments of U because U(VI)-aluminate solids have not been documented in the literature. These solids may not possess long range order and may have historically (if ever studied) been amorphous to XRD analysis. Our U-XAFS study results pertain to non-replicated bulk syntheses. The low levels of U in this sample make conclusions about higher shell behavior less straightforward than that which would be anticipated for studies with pure crystalline U solids such as that for uraninite [$U(IV)O_{2(s)}$]. Such studies with a more structurally pure U phase would be complex but better fits of the XAFS data would be expected.

XAFS data are representative of the average local environment, the eight U-U distances (ranging between 3 and 4 Å for schoepite) that exist with this solid are difficult to resolve in the FT data due to constructive and destructive interference between the oscillations associated with the eight different U-U interactions. The presence of multiple environments results in several overlapping shells, which creates difficulties when CN's and to a somewhat lesser degree, radial distances are sought during model fit analyses.
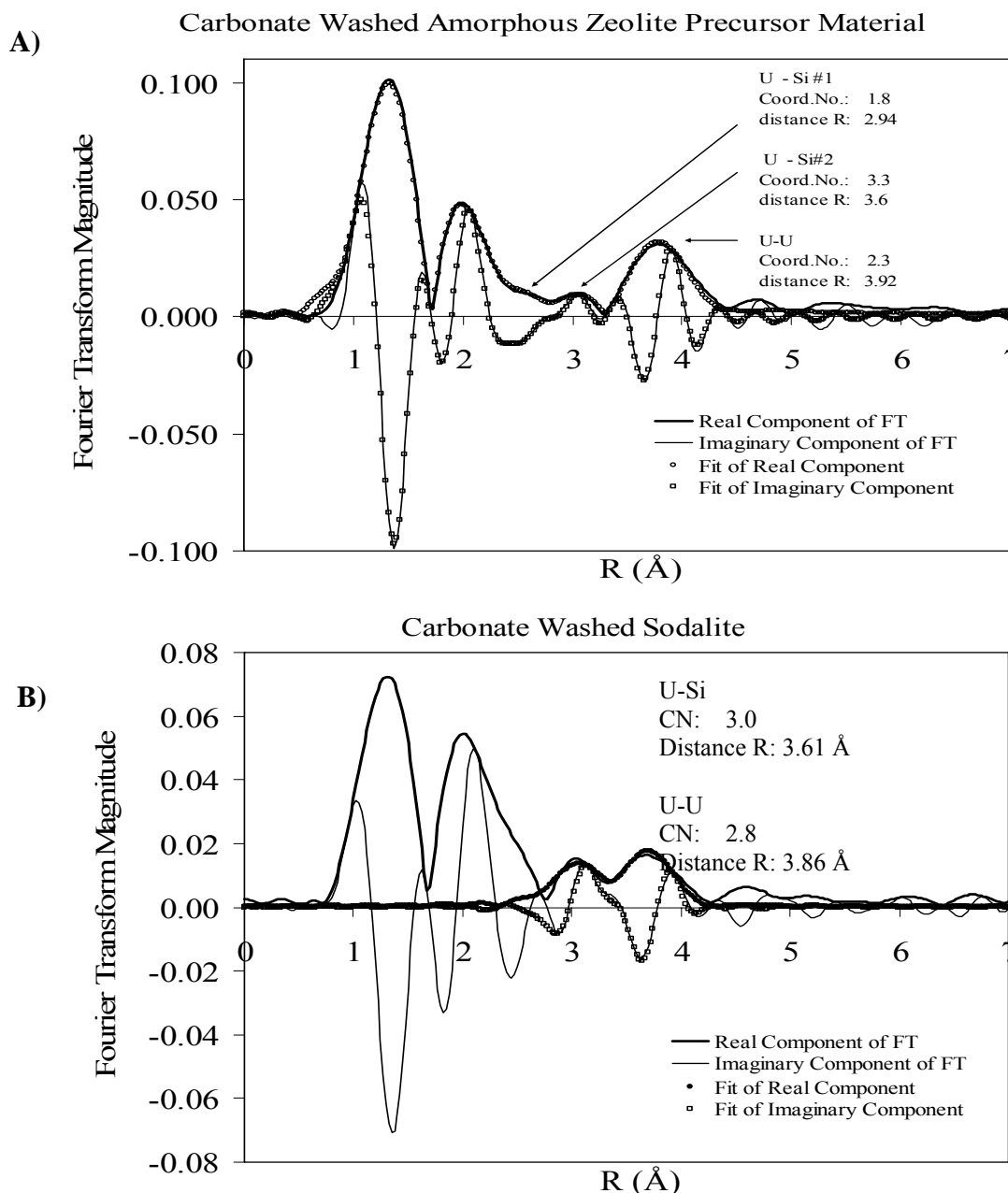
A)

Carbonate Washed Amorphous Zeolite Precursor Material

U - Si #1
Coord.No.:   1.8
distance R: 2.94

U - Si#2
Coord.No.:   3.3
distance R: 3.6

U-U
Coord.No.:   2.3
distance R: 3.92

Real Component of FT
Imaginary Component of FT
Fit of Real Component
Fit of Imaginary Component

R (Å)

Fourier Transform Magnitude

B)

Carbonate Washed Sodalite

U-Si
CN: 3.0
Distance R: 3.61 Å

U-U
CN: 2.8
Distance R: 3.86 Å

Real Component of FT
Imaginary Component of FT
Fit of Real Component
Fit of Imaginary Component

R (Å)

Fourier Transform Magnitude

Fig. 4 Model fits for the outer shell components of the FT data for (**A**) carbonate-washed amorphous zeolite precursor and (**B**) carbonate-washed sodalite.

DISCUSSION AND CONCLUSIONS

Discussion of the XAFS Data from the Unwashed, DI-washed and Na$_2$CO$_3$-washed NAS Solids

The XAFS data for the unwashed and DI-washed NAS solids showed evidence of outer coordination shell O, U and Si (data not shown)—suggesting that uranyl oxyhydroxide and uranyl silicate-like solids exist in these samples. However, we could not resolve CN or radial distance information from the recorded spectra due to the presence of multiple local environments for the U in these samples, which limited our ability to make more definitive interpretations of the XAFS data.

The XAFS data for the Na_2CO_3-washed samples exhibited characteristics that are indicative of fewer local U environments (i.e., possibly, a single U(VI) phase) as opposed to three or more as was probably present in the unwashed and DI-washed samples. The model fit data for the Na_2CO_3-washed sodalite and amorphous zeolite samples indicates that a uranyl-like silicate phase is present in the samples. This is because the U-Si radial distances are indicative of mostly corner-sharing U(VI) with SiO_4 tetrahedra (radial distances greater than 3.2 Å) and some edge-sharing U with SiO_4 tetrahedra (radial distances less than 3 Å). The absence of significant edge-sharing behavior supports the formation of uranyl silicates as opposed to sorbed U(VI) species on NAS because sorbed U(VI) typically attaches to aluminosilicate and silica-containing solids via edge-linking as shown in **Fig. 2A** and as discussed previously. The number of U-U interactions in the Na_2CO_3 -washed NAS samples suggests the precipitation of precursor material to a Na-weeksite and Na-boltwoodite type phase.

The precipitation of uranyl silicate and hydroxide phases could have occurred on the NAS surface or without the NAS surfaces. The XAFS data could not determine the nature of the precipitation (i.e., whether it was on NAS solids or not). However, the formation of a large amount of NAS solids relative to the low amount of U in the NAS solids could help seed the precipitation of U solids. Uptake of the U into the sodalite structure was possible, however, the uranyl silicate particles (which contain on average, several U atoms) that precipitated are clearly too large in size to exist in the sodalite structural cages or within the zeolite A tunnels. We estimate that the particle size (on average) of the precipitate material was colloidal in nature but too large to fit within the sodalite and zeolite frameworks. However, our XAFS data represent average radial distance and CN information. It is possible that small monomeric species may exist within the zeolite structures in addition to the presence of larger U polymeric species that are present outside of the zeolite structures. Because this U(VI)-silicate phase remains in the samples after leaching with DI water and Na_2CO_3, it is resistant to leaching. This stable (i.e., sparingly soluble) residual phase is most likely colloidal in nature and not likely to be detected by XRD analyses because of its short-range order. If formed in the 2H Evaporator, an amorphous uranyl silicate-type phase may convert to hydrated or dehydrated sodium diuranate with time or remain undetected.

Studies show that in the natural environment, which is typically less caustic than that of HLW, crystalline uranyl silicate solids are highly stable mineral phases in that they dissolve more slowly than other mineral phases under similar conditions. Uranophane $[Ca(H_3O)_2(UO_2)_2 (SiO_4)_2 \cdot 3H_2O]$ in particular has been identified as the most common U(VI) mineral in the environment, which suggests this mineral is fairly resistant to weathering in natural waters [58]. Dissolution studies have been done with uranyl silicates (uranophane and soddyite) in the presence of CO_3^{2-} [59, 60, 61]. Only one study has examined the effect of CO_3^{2-} concentration on uranyl silicate dissolution rates [60]. This study found that CO_3^{2-} increases the rate of soddyite dissolution. Another study examined the dissolution of schoepite and soddyite in 0.5 M Na_2CO_3 in batch. This study showed that schoepite dissolved 2.5 times faster than soddyite. The higher dissolution rate is thought to be due to the simplicity of the schoepite structure--relative to that of soddyite. For example, the U(VI) minerals with SiO_4 groups contain repeating units or "sheets" of tetrahedral group linkages whereas schoepite does not contain these linkages [58]. The silica tetrahedral linkages could be less prone to dissolution and therefore influence mineral dissolution rates. Hence, U(VI) solids such as schoepite, which do not have SiO_4 (silica tetrahedra) in their structures, are likely to be more soluble than minerals that have silica tetrahedra in their structures.

Many of our fits resulted in the generation of local first shell CNs that were inconsistent with that for known solid U species—such as the presence of two U-O axial distances and the low numbers of equatorial U-O CNs. Again, there are complexities associated with the multiple local environments. However, the radial distance information is more reliable than that of the CN values because for XAFS analyses, radial distance information is more readily obtained than that of CN information.

Discussion of the XAFS Data from the Si-free U Reference Solids
The XAFS data for the U phases from the Si-free U reference syntheses indicate that uranyl-type and uranate-type solids are formed. The presence of outer shell U in the FT data for suggests that the U precipitated during synthesis. The sodalite reference solids appear to contain Al—although no quantitative analyses for Al were performed. A more thorough verification of this would require more analyses and syntheses that are aimed at the study of U solids formation in Al-rich caustic solutions. The presence of multiple environments for U in these three samples limited our ability to make additional interpretations of the data.

The U-XAFS data for the precipitated solids from the U reference for the sodalite synthesis materials indicate potential bonding with Al (in the outer coordination shells). It is also possible that bonding with "tramp" Si (coming from the reagent chemicals used to make the salt solutions) rather than Al may have also occurred. The U-XAFS data for the Si-free U reference solid from the amorphous zeolite precursor preparation did not indicate the presence of Al bonding in the outer coordination shells. The absence of Al interactions may be due to the lower temperature (40 ^{o}C) used during these syntheses as opposed to the higher temperatures (80°C) that were used for the other syntheses (i.e., those for the reference U solids that were part of the sodalite syntheses).

In summary, the presence of Al and Si, U will precipitate during NAS formation as uranyl silicate and uranyl/ uranate oxyhydroxide phases, which have a highly amorphous behavior. Our studies yielded the following information:

- In general, the U(VI) that was removed from solution during these studies precipitated as two general forms: mainly U(VI)-oxide/hydroxide phases with minor amorphous U(VI)-silicates phases. The amorphous and colloidal U(VI)-silicate phases probably formed due to the high dissolved Si levels that were required for NAS precipitation. Although the U(VI)-silicates were the minor phases, they were the most stable phases because of their resistance to dissolution in the leaching solutions.

- The unwashed and DI-washed U-NAS precipitates that form in the presence of amorphous zeolite precursor material and sodalite possess *multiple* local coordination environments for the U. These environments consist of uranyl and uranate oxy(hydroxide) and uranyl silicate precipitate phases, which have a strong colloidal and amorphous character.

- For the DI-water and Na_2CO_3-washed samples, the average local environment of the U becomes less characteristic of multiple environments and more characteristic of an amorphous colloidal uranyl silicate phase than of a uranyl oxyhydroxide phase. This uranyl silicate material has bonding characteristics of uranyl silicate minerals but no identifications to known U(VI)-silicate minerals could be made. Follow-up studies to determine the solubility of this phase will be complicated due to the colloidal nature of the uranyl silicate materials.

- For these DI-water and Na_2CO_3-washed samples, the presence of Si at distances that are representative of corner-sharing [of silicate tetrahedra (SiO_4) with U(VI) polyhedra] behavior indicate that U(VI) exists in a solid phase precipitate form as opposed to sorbed on the NAS. We cannot determine whether there is a seeding relationship between the U and NAS solids from our data or whether these solids did not dissolve in the wash solutions due to their occlusion by NAS solids.

Studies to characterize U solids that have been synthesized from high pH U and Si containing solutions are on-going in addition to the XAFS-based characterization of archived 2H Evaporator scale. Further study is recommended to evaluate the potential for the formation of U-Al solid phases in the absence of added Si and to characterize U solids that will form in high Si and Al caustic salt solutions or U-NAS solids that form during the precipitation of the zeolite called cancrinite. A study of the influence of Si on U(VI) solubility under alkaline conditions with temperature is recommended because little information exists about U under these conditions. Finally, if tank farm waste containing elevated levels of Pu were to be evaporated, studies on the formation and characterization of Pu silicate phases would also be recommended.

ACKNOWLEDGEMENTS

REFERENCES

1   W. STUMM, Chemistry of the Solid-Water Interface: Processes at the Mineral-Water and Particle-Water Interface in Natural Systems. Wiley-Interscience, NY (1992).

2   M. B. MCBRIDE, Environmental Chemistry of Soils. Oxford Press, NY (1994).

3   M. T. OLGUIN et al., "Characterization of UO_2^{2+}-exchanged Y zeolite," J. Radio. Anal. Nucl. Chem. **222**, 235-237 (1997).

4   Y. LI and P. C. BURNS, "The structures of two sodium uranyl compounds relevant to nuclear waste disposal," J. Nucl. Mater. **299**, 219-226 (2001).

5   D. T. HOBBS, M. G. BRONIKOWSKI, T. B. EDWARDS, and R. L. PULMANO, "Final Report on Phase III Testing of Monosodium Titanate Adsorption," WSRC-TR-99-00134 (1999).

6   M. C. DUFF, D. T. HOBBS, and S. D. FINK, "Permanganate Treatment Optimization Studies for Strontium and Actinide Removal from High Level Waste Simulants," WSRC-TR-2002-0027 (2002).

7   M. T. CRESPO, J. L. GASCON, and M. L. ACENA, "Techniques and analytical methods in the determination of uranium, thorium, plutonium, americium and radium by adsorption on manganese dioxide," Sci.Tot.Environ. **130**, 383-391 (1993).

8   M. C. DUFF, D. B. HUNTER, D. T. HOBBS, A. JURGENSEN, and S. D. FINK, "Characterization of Sorbed Plutonium, Neptunium, Strontium on Manganese Solids from Permanganate Reduction," WSRC-TR-2002-00366, Rev. 0 (2002).

9   D. L. CLARK et al., "Chemical speciation of the uranyl ion under highly alkaline conditions, synthesis, structures and oxo ligand exchange dynamics," Inorg. Chem. **38**, 1456-1466 (1999).

10 C-K.D. HSI and D. LANGMUIR, "Adsorption of uranyl onto ferric oxyhydroxides: Applications of the surface complexation site-binding model," Geochim. Cosmochim. Acta **49**, 1931-1941 (1985).

11 M. C. DUFF and C. AMRHEIN, "Uranium(VI) adsorption on goethite and soil in carbonate solutions,". Soil Sci. Soc. Amer. J. **743,** 1393-1400 (1996).

12 M. C. DUFF, D. B. HUNTER, D. T. HOBBS, M. J. BARNES, and S. D. FINK, "Characterization of Sorbed Uranium, Plutonium and Neptunium on Monosodium Titanate," WSRC-TR-2001-00356 (2001).

13 S. AKYIL, M. A. A. ASLANI, Ş. ŎLMEZ, and M. ERAL, "Kinetic studies of uranium(VI) adsorption on a composite ion exchanger," J. Radioanal. Nucl. Chem. Lett. **213**, 441-450 (1996).

14 F. Z. EL AAMRANI, L. DURO, J. DE PABLO, and J. BRUNO, "Experimental study and modeling of the sorption of uranium(VI) onto olivine rock," Appl. Geochem. **17**, 399-408 (2002).

15 S. AKYIL, M. A. A. ASLANI, and Ş. AYTAŞ, "Distribution of uranium on zeolite X and investigation of thermodynamic parameters for this system," J. Alloys Cpds **271/273**, 769-773 (1998).

16 J. PRIKRYL, A. JAIN, D. R. TURNER, and R. T. PABALAN, "Uranium(VI) sorption behavior on silicate mineral mixtures," J. Contam. Hydrol. **47**, 241-253 (2001).

17 M. E. D. G. AZENHA, M. GRAÇA MIGUEL, S. J. FORMOSINHO, and H. D. BURROWS, "The characterization by luminescence spectroscopy of uranium(VI) incorporated into zeolites and aluminas," J. Molec. Structure **563-564**, 439-442 (2001).

18 D. C. KONINGSBERGER and R. PRINS, X-ray Absorption: Techniques of EXAFS, SEXAFS and XANES, Wiley, New York. (1988).

19 E. A. STERN, "Theory of extended X-ray absorption fine structure,"Phys. Rev. **B10**, 3027-3037 (1974).

20 M. C. DUFF, J. U. COUGHLIN, and D. B HUNTER, "Uranium co-precipitation with Fe oxide minerals," Geochim. Cosmochim. Acta **66**, 3533-3547 (2002).

21 K. H. LIESER, S. QUANDT-KLENK, and B. THYBUSCH, "Sorption of uranyl ions on hydrous silicon dioxide," Radiochim. Acta **57**, 45-50 (1992).

22 A. MENSAH, J. LI, and M. ZBIK, "The Chemistry, Crystallization, Physicochemical Properties and Behavior of Sodium Aluminosilicate Solid Phases," WSRC/ERDA GA00083 (2002).

23 L. N. OJI and A. L. WILLIAMS, "Evaluation of the Incorporation of Uranium into Sodium Aluminosilicate Phases (U)," WSRC-2002-TR-00527, Rev. 0 (2002).

24 T. RESSLER, "WinXAS. A program for X-ray absorption spectroscopy data analysis under MS Windows," J. Synchr. Rad. **5**, 118-122 (1999).

25 M. NEWVILLE, P. LIVINS, Y. YACOBY, J. J. REHR, and E. A. STERN, "Near-edge X-ray-absorption fine-structure of Pb – A comparison of theory and experiment," Phys. Rev. B-Cond. Matter, **47**, 14126-14131 (1993).

26 D. E. SAYERS and B. A. BUNKER, In "X-ray Absorption: Techniques of EXAFS, SEXAFS and XANES," Koningsberger, D. C. and Prins, R. (eds). Wiley, New York, Chap. 6. (1988).

27 J. MUSTRE DE LEON, J. J. REHR, S. I. ZABINSKY, and R. C. ALBERS, "Ab initio curved-wave x-ray-absorption fine structure, Phys. Rev. **B44**, 4146 (1991).

28 J. J. REHR and R. C. ALBERS, "Scattering-matrix formulation of curved-wave multiple-scattering theory: Application to x-ray-absorption fine structure," Phys. Rev. **B41**, 8139 (1990).

29 J. J REHR, J. MUSTRE DE LEON, S. I. ZABINSKY, and R. C. ALBERS, "Theoretical X-ray absorption fine structure standards," J. Am. Chem. Soc**. 113**, 5135 (1991).

30 J. J REHR, S. I. ZABINSKY, and R. C. ALBERS, "High-order multiple scattering calculations of x-ray-absorption fine structure," Phys. Rev. Let. **69**, 3397 (1992).

31 E. A. STERN, M. NEWVILLE, B. RAVEL, Y. YACOBY, and D. HASKEL, "The UWAFS analysis package - Philosophy and details," Physica B. **208-209**, 117-120 (1995).

32 L. N. MOYES, et al., "Uranium uptake from aqueous solution by interaction with goethite, lepidocrocite, muscovite, and mackinawite: An X-ray absorption spectroscopy study," Env. Sci. Technol. **34,** 1062-1068 (2000).

33 E. A. HUDSON, et al., "The structure of U^{6+} sorption complexes on vermiculite and hydrobiotite," Clays Clay Min. **47**, 439-457 (1999).

34 C. CHISHOLM-BRAUSE, S. D. CONRADSON, C. T. BUSCHER, P. G. ELLER, and D. E. MORRIS, "Speciation of uranyl sorbed at multiple binding sites on montmorillionite," Geochim. Cosmochim. Acta**. 58**, 3625-3631 (1994).

35 T. D. WAITE, J. A. DAVIS, T. E. PAYNE, G. A. WAYCHUNAS, and N. XU, "Uranium adsorption to ferrihydrate: Application of a surface complexation model," Geochim. Cosmochim. Acta. **58**, 5465-5478 (1994).

36 P. WERSIN, M. F. HOCHELLA, J. PERSSON, G. REDDEN, J. O. LECKIE, and D. W. HARRIS, "Interaction between aqueous uranium(VI) and sulfide minerals: Spectroscopic evidence for sorption and reduction," Geochim. Cosmochim. Acta **58**, 2829-2843 (1994).

37 J. R. BARGAR, R. REITMEYER, and J. A. DAVIS, "Spectroscopic confirmation of uranium(VI)-carbonato adsorption complexes on hematite," Env. Sci. Technol. **33**, 2481-2484 (1999).

38 E. R. SYLWESTER, E. A. HUDSON, and P. G. ALLEN, "The structure of uranium(VI) sorption complexes on silica, alumina and montmorillonite," Geochim. Cosmochim. Acta. **64**, 2431-2438 (2000).

39 K. H. LIESER, S. QUANDTKLENK, and B. THYBUSCH, "Sorption of uranyl ions on hydrous silicon dioxide," Radiochim. Acta **57**, 45-50 (1992).

40 J. R. BARGAR, R. REITMEYER, J. J. LEHNART, and J. A. DAVIS, "Characterization of U(VI)-carbonato ternary complexes on hematite: EXAFS and electrophoretic mobility measurements," Geochim. Cosmochim. Acta**. 64**, 2737-2749 (2000).

41 P. G. ALLEN, et al., "Determinations of uranium structures by EXAFS: Schoepite and other U(VI) oxide precipitates," Radiochim. Acta **75**, 47-53. (1996).

42 H. A. THOMPSON, G. E. BROWN, and G. A. PARKS, "XAFS spectroscopic study of uranyl coordination in solids and aqueous solution," Amer. Mineral. **82**, 483-496 (1997).

43 T. ALLARD, P. ILDEFONSE, C. BEAUCAIRE, and G. CALAS, "Structural chemistry of uranium associated with Si, Al, Fe gels in a granitic uranium mine," Chem. Geol. **158**, 81-103 (1999).

44 N. C. STURCHIO, M. R. ANTONIO, L. SODERHOLM, S. R. SUTTON, and J. C. BRANNON, "Tetravalent uranium in calcite," Science **281**, 971-973 (1998).

45 R. J. REEDER, M. NUGENT, C. D. TAIT, and D. E. MORRIS, "Uranyl incorporation into calcite and aragonite: XAFS and luminescence studies," Env. Sci Technol. **34**, 638-644 (2000).

46 G. D. TURNER, J. M. ZACHARA, J. P. MCKINLEY, and S. C. SMITH, "Surface-charge properties and UO_2^{2+} adsorption of a subsurface smectite," Geochim. Cosmochim. Acta. **60,** 3399-3414 (1996).

47 J. M. ZACHARA and J. P. MCKINLEY, "Influence of hydrolysis on the sorption of metal cations by smectites: Importance of edge coordination reactions," Aquatic Sciences. **55**, 250-261 (1993).

48 P. C. BURNS, "The Crystal Chemistry of Uranium. In: Uranium: Mineralogy, Geochemistry and the Environment," Reviews in Mineralogy **38**, pp. 23-90, Mineral. Soc. Amer. (1999).

49 P. C. BURNS, R. C. EWING, and F. C. HAWTHORN, "The crystal chemistry of hexavalent uranium: Polyhedral geometries, bond-valence parameters, and polymerization of polyhedra," Can. Mineral. **35**, 1551-1570 (1997).

50 V. WHEATON, D. MAJUMDAR, K. BALASUBRAMANIAN, L. CHAUFFE, and P. G. ALLEN, "A comparative theoretical study of uranyl silicate complexes," Chem. Phys. Lett. 371, 349-359 (2003).

51 T. REICH, et al, "An EXAFS study of uranium(VI) sorption onto silica gel and ferrihydrite," J. Electron Microsc. Related Phenomenon **96**, 237-243 (1998).

52 T. REICH, et al., "Characterization of hydrous uranyl silicate by EXAFS," Radiochim. Acta **74**, 219-223 (1996).

53 M. C. DUFF, D. B. HUNTER, M. J. BARNES, and S. D. FINK, "Characterization of Uranium and Mercury Speciation in High Level Waste Tank 8F and 11H Sludge," WSRC-TR-2001-00428, Rev. 0. (2002).

54 T. R. GRIFFITHS and V. A. VOLKOVICH, "A review of the high temperature oxidation of uranium oxides in molten salts and in the solids state to form alkali metal uranates, and their composition properties," J. Nucl. Mater. **274**, 229-251 (1999).

55 F. FARGES, C. W. PONADER, G. CALAS, and G. E. Jr. BROWN, "Structural environments of incompatible elements in silicate glass/melt systems: II. U^{IV}, U^{V}, and U^{VI}," Geochim. Cosmochim. Acta **56,** 4205-4220 (1992).

56 D. T. HOBBS and T. B. EDWARDS, "Solubility of Uranium in Alkaline Salt Solutions," WSRC-TR-93-00454. (1993).

57 D. T. HOBBS, T. B. EDWARDS, and S. D. FLEISCHMAN "Solubility of Plutonium and Uranium in Alkaline Salt Solutions," WSRC-TR-93-00056 (1993).

58 D. K. SMITH, "Uranium Mineralogy," In Uranium Geochemistry, Mineralogy, Exploration and Resources (ed. B. DEVIVO, F. IPPOLITO, G. CAPALDI, and P. R. SIMPSON). pp. 43-88. Inst. Mining and Metallurgy. (1984).

59 I. PÉREZ, I. CASAS, M. MARTÍN, and BRUNO, J., "The thermodynamics and kinetics of uranophane dissolution in bicarbonate test solutions," Geochim. Cosmochim. Acta **64,** 603-608 (2000).

60 I. PÉREZ, I. CASAS, M. TORRERO, E. CERA, L. DURO, and J. BRUNO, "Dissolution Studies of Soddyite as a Long-Term Analogue of the Oxidative Alteration of the Spent Nuclear Fuel Matrix," Scientific Basis for Nuclear Waste Management XXI. MRS Sympos. Proceedings, **465**, 565-572. Pittsburgh, PA, Material Res. Soc. (1997).

61 C.F.V. MASON, M. C. DUFF, J. A. MUSGRAVE, and W. RUNDE, "Interim Report on Remedial Actions for Yuma Catch Box Sand," Los Alamos National Lab., Los Alamos, NM, LA-UR 96-3485 (1996).